

Index

$1/f$ noise, 248
1D LiDAR, 8

2D imaging, 3
2D LiDAR, 8, 432

3D imaging, 3
3D mapping LiDAR, 452

A

acousto-optic modulator (AOM), 288
Aeolian Dust Experiment on Climate (ADEC), 58
airborne laser bathymetry (ALB), 70
Airy disk, 389
American Society for Photogrammetry Engineering and Remote Sensing (ASPRS), 121
analog-to-digital (A/D) converter, 190
antenna gain, 182
Asian Dust LiDAR Observation Network (AD-Net), 58
ASPRS Accuracy Standards for Digital Geospatial Data, 121
asynchronous readout, 290
atmospheric attenuation, 466
Atmospheric Laser Doppler Instrument (ALADIN), 44
auto LiDAR, 452
Autonomous Terminal Homing (ATH), 41

autonomous underwater vehicle (AUV), 69
avalanche photodiode (APD), 65, 233

B

background noise, 242
backscatter, 470
beam divergence, 87, 331
Beer's law, 466
binomial distribution, 275
birefringence, 332
birefringent crystals, 214
bistatic LiDAR, 18
blackbody, 242
blackbody radiation, 3
Boeing SpectraLab, 75
Boltzmann's constant, 240

C

carrier-to-noise ratio (CNR), 285
catastrophic optical destruction (COD), 206
central limit theorem, 238
circular polarization, 284
CLARA, 39
CO₂ laser, 28
CO₂ LiDAR, 38
coherence, 178
coherent detection, 112
coherent LiDAR, 3
compressive sensing, 442
conditional probability, 275

- Continuously Operating Reference Station (CORS), 121
 Cr:ZnSe, 211
 cross-section, 94
 Cruise Missile Advanced Guidance (CMAG), 41
 crystalline quartz (SiO₂), 213
 cumulative distribution function (CDF), 398
 Curie temperature, 356
- D**
 dark current, 248
 dark current nonuniformity, 417
 deformable mirror (DM), 104
 detector angular subtense (DAS), 8
 differential absorption LiDAR (DIAL), 58
 digital elevation model (DEM), 127
 digital holography, 12
 digital terrain elevation data (DTED), 436
 diode lasers, 184, 203
 direct-detection LiDAR, 184
 Doppler LiDAR, 415
 Doppler shift, 3, 288, 393
 dual-frequency liquid crystal (DFLC), 333
- E**
 Ecole Polytechnique, France, 44
 edge-emitting diode lasers, 203
 eigenmodes, 441
 electro-optic crystal, 195, 343
 electron-bombarded active-pixel sensor (EBAPS), 117
 electron-initiated avalanche photodiode (e-APD), 117
 electrowetting, 338
 ERASER, 64
 erbium doping, 222
- F**
 fast-steering mirror (FSM), 313
 Federal Emergency Management Agency (FEMA), 131
 Federal Geographic Data Committee (FGDC), 127
 ferroelectric liquid crystals, 337
 fiber lasers, 184, 211
 field of view (FOV), 8
 fixed liquid crystal polarized grating (LCPG), 365
 fixed-pattern noise (FPN), 416–417
 flash illumination, 479
 flashlamps, 194
 flicker noise, 248
 focal spot, 368
 foliage poke through, 66
 Forward Combat System (FCS), 67
 four-level laser, 193
 Fourier transform, 399, 430
 frame rate, 462
- G**
 GaAs photocathode, 117
 gas lasers, 184
 gate time, 238
 gated active 2D imaging, 64
 Gaussian beam, 13, 87
 Gaussian distribution, 238
 Geiger-mode avalanche photodiode (GMAPD), 19, 65, 236
 Geiger-mode LiDAR (GML), 120
 general image quality equation (GIQE), 437
 geographic information system (GIS), 131
 ghost-imaging LiDAR, 293
 gimbals, 309
 Global Navigation Satellite System (GNSS), 121
 Global Positioning System (GPS), 121

grayscale, 3, 9, 239

ground sample distance (GSD),
436, 93–94

H

heterodyne detection, 237

heterodyne mixing efficiency, 282

HgCdTe APD, 250

high range resolution, 114

holographic optical element
(HOE), 92

human visibility, 429

hydrography, 70

I

ideal point response (IPR), 410

image metrics, 425

individual transmit/receive (T/R)
module, 326

inertial measurement unit
(IMU), 396

Infrared Airborne Radar
(IRAR), 61

InGaAs LMAPD, 254

InGaAs photocathode, 117

inphase component of a beam, 283

integrated sidelobe ratio
(ISLR), 411

interband cascade laser (ICL), 210

interband diode lasers, 203

intermediate frequency (IF), 190, 236

Intevac's LIVAR[®] 4000 laser-gated
viewer, 68

Intevac's LIVAR[®] M506, 116

inverse synthetic-aperture LiDAR
(inverse SAL), 149

irradiance, 9

isolation, 18

J

Jigsaw 3D LiDAR, 66

Johnson criteria, 425, 461

Jones calculus, 364

K

K(TiO)AsO₄ (KTA), 220

Kerr effect, 195, 341

Kinetic Energy Interceptor, 51

KTN, 345

KTP, 220

L

ladar, 7

Lambertian scattering, 95, 247

Laser Airborne Depth Sounder
(LADS), 71

laser rangefinder, 30

laser vibrometry, 142, 394,
452, 477

laser-induced breakdown
spectroscopy (LIBS), 11, 136

laser-induced fluorescence (LIF)
LiDAR, 136

lasers, 178

LATAS (Laser True Airspeed
System), 39

least significant bit (LSB), 239

lenslet, 322

LiDAR, 1

linear frequency modulation
(LFM), 379

linear frequency-modulated
waveform, 188

linear polarization, 284

linear-mode avalanche photodiode
(LMAPD), 19, 236

Lissajous figure, 315

local oscillator (LO), 3

LOCUS (Laser Obstacle and Cable
Unmasking System), 39

Loitering Attack Missile
(LAM), 67

longitudinal modes, 197

longwave infrared (LWIR), 100

Low Altitude Navigation and
Targeting Infrared for Night
(LANTIRN), 65

Low Cost Autonomous Attack System (LOCAAS), 66
 LOWKATER, 53

M

master oscillator power amplifier (MOPA), 200
 maximum permissible exposure (MPE), 15, 464
 micro-Doppler, 284
 micro-electromechanical system (MEMS), 320
 microlens array, 324
 microscan, 390, 461
 Microsoft[®] Kinect game system, 10
 midwave infrared (MWIR), 100
 Mie scattering, 101
 MIT Lincoln Lab, 32
 MIT/Lincoln Lab Firepond system, 38
 mode-locked lasers, 198
 Modular Optical Aperture Building Blocks (MOABB), 338
 modulation transfer function (MTF), 433
 modulation transfer function compensation (MTFC), 438
 modulo 2π beam steering, 328
 monostatic LiDAR, 17
 MONITOR (Methane Observation Networks with Innovative Technology to Obtain Reductions), 11
 multipixel–photon-counter (MPPC), 279
 multiple-input, multiple-output (MIMO), 5, 10, 150
 multiple–line-of-collection (LOC), 476

N

NASA Goddard Space Flight Center, 32

National Cooperative Highway Research Program (NCHRP), 132
 National Digital Elevation Program (NDEP), 127
 National Geospatial Agency (NGA), 396
 National Imagery Interpretability Rating Scales (NIIRS), 425, 433
 National Institute for Environmental Studies (NIES), Japan, 61
 National Spatial Reference System (NSRS), 123
 Nd:YAG laser, 28
 negative binomial distribution, 239
 noise-equivalent photons (NEPh), 117
 noise-equivalent vibration velocity (NEVV), 411
 Nyquist sampling, 385

O

Open Geospatial Consortium (OGC), 127
 operational obstacle avoidance system, 36
 optical coherence tomography (OCT), 71
 optical parametric amplifier (OPA), 212
 optical parametric oscillator (OPO), 199, 67, 212
 optical path difference (OPD), 309
 optical phased array (OPA), 309
 orientation-patterned GaAs (OP-GaAs), 221

P

passive EO sensors, 3
 Pave Tack pod, 65
 peak sidelobe ratio (PSLR), 411

periodically poled lithium niobate (PPLN), 213
photomultiplier tube (PMT), 279
PMN-PT, 345
Pockels cell, 195, 341
point spread function (PSF), 8, 389
Poisson distribution, 239
polygon scanner, 320
Princeton Lightwave, 75
pseudo-random-coded waveform, 188

Q

Q switch, 184
Q-switched laser, 199
Q-switched Nd:YAG laser, 31
quadrature components of a beam, 283
quadrature detection, 283
quantum cascade laser (QCL), 184, 208
quantum efficiency, 237
Quiet Knight, 43

R

Raleigh scattering, 101
Raman LiDAR, 11, 57
range accuracy, 388
range-gated active imaging (2D LiDAR), 116
range imaging, 462
range precision, 388
range resolution, 388
range walk, 415, 418
readout integrated circuit (ROIC), 67
relative edge response (RER), 437
Risley prism, 315
root-mean-square error (RSME), 127
rotating polygon, 318
Royal Signals and Radar Establishment (RSRE), 39

S

SBN, 352
scale-invariant feature transform (SIFT), 442
scanning LiDAR, 464
separate absorption and multiplication (SAM) region, 270
separate absorption, charge, and multiplication (SACM), 253
shot noise, 241
signal-to-noise ratio (SNR), 19, 237
silicon detectors, 279
single-photon avalanche diode (SPAD), 279
single-photon LiDAR (SPL), 120
solid state lasers, 178
space-fed, phased-array steering, 326
spatial coherence, 178
spatial fly-back region, 334
speckle, 104
speckle imaging LiDAR, 143
spurious sidelobe ratio (SSLR), 411
Standoff Precision Identification in Three Dimensions (SPI-3D), 66
steerable electro-evanescent optical refractor (SEEOR), 336
stimulated Brillouin scattering (SBS), 224
Stokes parameter, 365
Strategic Defense Initiative Organization (SDIO), 51
super-Gaussian beam, 13, 87
synthetic-aperture LiDAR (SAL), 10, 146, 4, 433
synthetic-aperture radar (SAR), 4, 50

T

temporal coherence, 178
temporal heterodyne detection, 12, 281
Thanh Hoa Bridge (aka Dragon's Jaw), Vietnam, 36
thermal noise, 240

thermoelectrical (TE) cooling, 271
three-level laser, 192
thulium-doped silica fiber
 lasers, 226
Ti:sapphire laser, 190
time–bandwidth product, 186
time over threshold (TOT), 279
topo-bathymetric LiDAR, 135

U

U.S. Geological Survey (USGS)
 National Geospatial Program
 (NGP), 445
U.S. Geological Survey (USGS)
 LiDAR Base Specifications, 121
unambiguous range, 386, 412
Universal Transverse Mercator
 (UTM), 124

unmanned aerial vehicle (UAV), 69

V

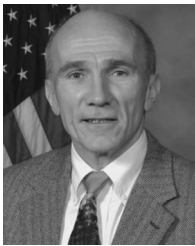
vertical-cavity, surface-emitting
 laser (VCSEL), 207
Video Guidance Sensor (VGS), 51
volume holographic gratings, 367

W

wide-area mapping (WAM), 476
wind sensing, 28, 481
World Geodetic System
 (WGS84)-based spatial
 referencing, 124

Z

ZnGeP₂ (ZGP), 220



Dr. **Paul F. McManamon** started Exciting Technology LLC after he retired from being Chief Scientist for the Air Force Research Lab (AFRL) Sensors Directorate. He is also Technical Director of the Lidar and Optical Communications Institute (LOCI) at the University of Dayton. He chaired the 2014 U.S. National Academy of Sciences Study “Laser Radar: Progress and Opportunities in Active Electro-Optical Sensing.” He was the main LiDAR expert witness for Uber in the lawsuit Uber versus Google/Waymo. He cochaired the 2012 U.S. NAS study “Optics and Photonics, Essential Technologies for Our Nation,” which recommended a National Photonics Initiative (NPI). Dr. McManamon was also vice chair of the 2010 NAS study “Seeing Photons: Progress and Limits of Visible and Infrared Sensor Arrays.”

Dr. McManamon is a Fellow of SPIE, IEEE, OSA, AFRL, the Directed Energy Professional Society (DEPS), the Military Sensing Symposia (MSS), and the American Institute of Aeronautics and Astronautics (AIAA). Dr. McManamon received the IEEE W.R.G. Baker Award in 1998 for the best paper in *any* refereed IEEE journal or publication (>20,000 papers). He was president of SPIE in 2006. He served on the SPIE Board of Directors for seven years and on the SPIE Executive Committee from 2003 through 2007. Dr. McManamon worked with Dr. Fenner Milton and Dr. Gerry Trunk to found the MSS, combining IRIS and the Tri-Service Radar Symposia. He worked as a civilian employee of the Air Force at WPAFB from May 1968 through May 2008. His last position for the Air Force was chief scientist for the AFRL Sensors Directorate, where he was responsible for the technical aspects of all AFRL sensing technologies, including RF and EO sensing, automatic object recognition, infrared countermeasure (IRCM), electronic warfare, and device technologies. Prior to that, he also was senior scientist for EO/IR Sensors, and acting chief scientist for the Avionics Directorate for >2.5 years. In 2006 he received the Presidential Rank Award of Meritorious Executive. He was the co-recipient of the SPIE President’s Award in 2013.